

Physics Fun with Discrete Scale Invariance

Howard Georgi,*

Center for the Fundamental Laws of Nature

The Physics Laboratories

Harvard University

Cambridge, MA 02138

06/16

Abstract

I construct a quantum field theory model with discrete scale invariance at tree level. The model has some unusual mathematical properties (such as the appearance of q -hypergeometric series) and may possibly have some interesting physical properties as well. In this note, I explore some possible physics that could be regarded as a violation of standard effective field theory ideas.

arXiv:1606.03405v1 [hep-ph] 10 Jun 2016

*hgeorgi@fas.harvard.edu

1 Introduction

In this note, we discuss a simple (though infinitely large) quantum field theory that has a formal discrete scale invariance in tree approximation. The original motivation (probably not successfully realized) was to get some insight into theories in which the standard model communicates with a conformal sector. But this construction leads to interesting mathematics and perhaps to some interesting physics. A wildly optimistic hope is that studying this simple model might yield insights into the hierarchy puzzle. In this note, we will focus on the physics, and relegate some amusing mathematical results to [1].

The finite version of our model has been considered before (see for example [2, 3, 4, 5, 6, 7]) as a discretization of a warped extra dimension to study important physical effects like the running of couplings. We hope that our explicit results in the infinite theory may be useful for these important applications.

In section 2, we introduce the field theory model and make the connection with a system of springs and masses. In section 3, we analyze the gauge couplings of the mass-eigenstate massive vector bosons. In section 4, we discuss one way of thinking about the infinite theory as a limit of finite theories, and we continue in section 5 to discuss how the approach to the limit depends on boundary conditions. In section 6, we will suggest that the dependence on boundary conditions can be much larger than predicted in a naive effective theory picture.

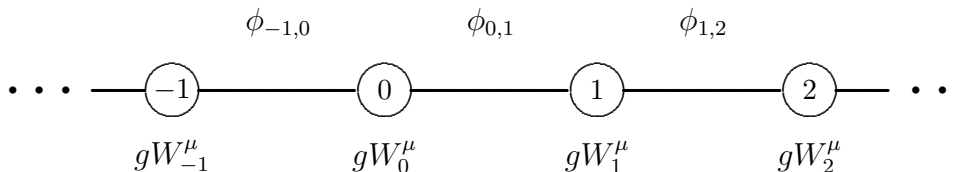


Figure 1: A deconstructed dimension..

2 Discrete Scale Invariance

We start with a deconstructed dimension as an infinite, linear moose described in the notation of [8] by the diagram shown in figure 1. This describes a series of $SU(N)$ groups labeled by the integers in the circles and scalars transforming like $\phi_{j,j+1} \sim (N, \bar{N})$ under $SU(N)_j \times SU(N)_{j+1}$ described by the solid lines between neighboring circles, as shown in figure 1. The gauge couplings are all assumed to equal g and the gauge fields are W_j^μ .

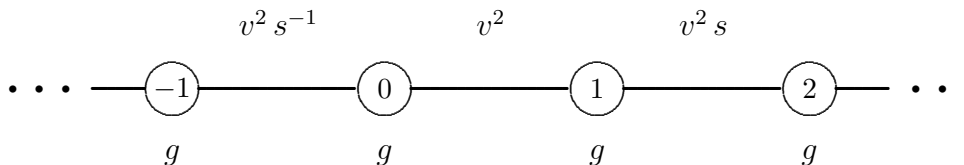


Figure 2: A discretely scale invariant system.

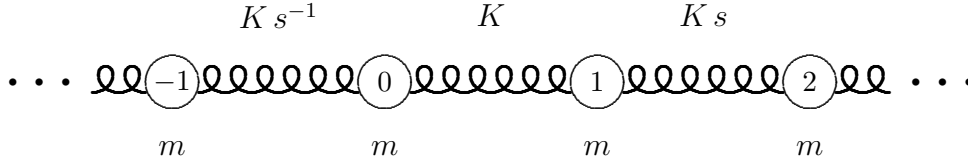


Figure 3: The mechanical analog of the system in figure 2.

But the unusual thing we will do here is to assume that the expectation values of the fields grow exponentially with j

$$\langle \phi_{j,j+1} \rangle = v s^{j/2} \quad (2.1)$$

where s is a positive number. This form obviously has a discrete scale invariance under a combination of rescaling by $s^{1/2}$ and translating one unit in j . The expectation value (2.1) can in fact arise at tree level from a scalar potential with the same discrete scale invariance. We don't expect this discrete scale invariance to survive beyond tree approximation in this model. But I believe that the structure of the massive gauge bosons and couplings may be interesting as an illustration of some general principles.

And besides, it is fun, because this model can be mapped onto the longitudinal oscillations of the system of masses and springs shown in figure 3.

The correspondance is this. If $K \rightarrow v^2$ and $m \rightarrow 1/g^2$, the angular frequencies of the normal modes of the system ω_α are proportional to the masses of the heavy gauge bosons, M_α .

For $s = 1$, this is just the familiar system in which the normal modes are infinite waves and the massive vector bosons are delocalized — spread over all j as in a deconstructed dimension. [9] However (as was noted qualitatively in [3] for the field theory) unlike the situation with $s = 1$, the normal modes for $s \neq 1$ are not infinitely spread out. They go to zero for $j \rightarrow \pm\infty$ and for very large or very small s , each mode is localized around one block.

For large s , it is very plausible that there is a mode in which block 0 oscillates with $\omega \approx \omega_0 = \sqrt{K/m}$. It is worth thinking qualitatively about the physics of this for large s , where the strength of the springs increases as we go to the right, for increasing j . For an oscillation with $\omega \approx \omega_0$, block 1 is nearly stuck in place by the stiff spring to its right. The oscillation of block 0 is primarily due to the spring on its right, and block 0 barely feels the effect of the weak spring to its left. So we expect that as $s \rightarrow \infty$, there will be a mode in which block 0 oscillates with $\omega \rightarrow \omega_0$ while the displacements of all the other blocks go to zero. For large but finite s , the displacements in this mode drop off away from $j = 0$. To the right, for $j > 0$, the displacements fall off exponentially. One can think of each spring driving the block to its right below resonance, so all the displacements are in phase. To the left, for $j < 0$, the displacements oscillate in sign, because the blocks are driven above resonance by the springs to their right.

It is straightforward to turn this physical picture into a perturbative calculation in $1/s$, and the result is a bit surprising. The first surprise is that ω is **exactly equal** to ω_0 for any $s \neq 1$. Using the perturbative result that there is a mode with $\omega = \omega_0$, we can write a

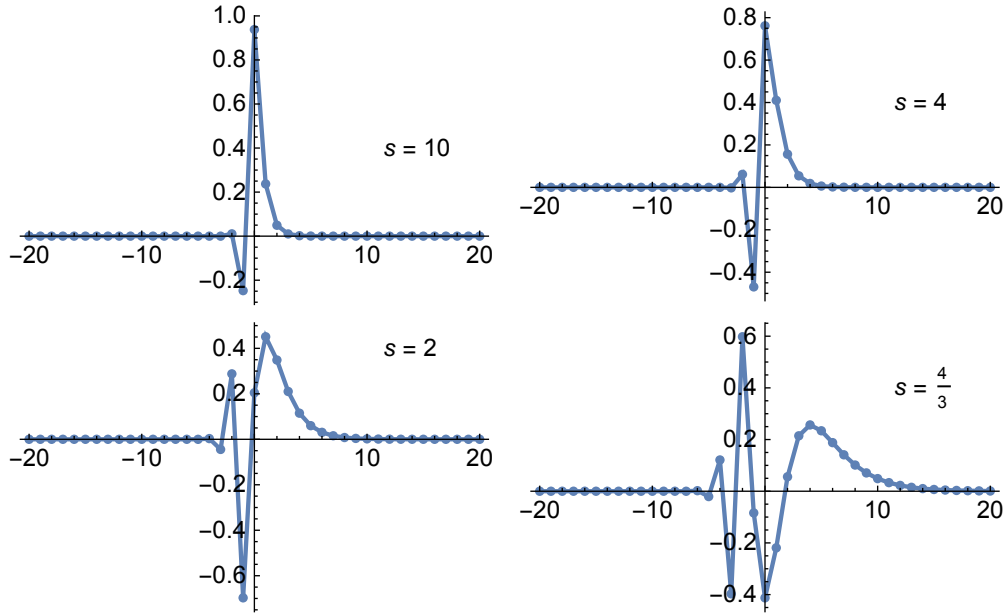


Figure 4: The amplitudes for the $\omega = \omega_0$ mode versus j for various values of s .

recursion relation for the displacement $\psi_j(s)$ of the j th block in this mode very simply as

$$s^j \left(\psi_j(s) - \psi_{j+1}(s) \right) + s^{j-1} \left(\psi_j(s) - \psi_{j-1}(s) \right) - \psi_j(s) = 0 \quad (2.2)$$

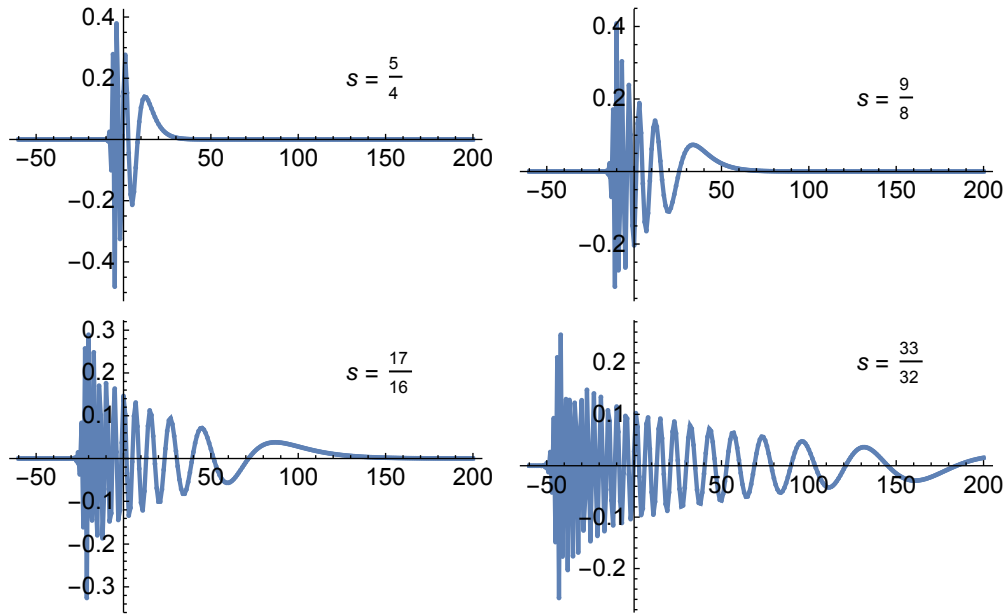


Figure 5: The amplitudes for the $\omega = \omega_0$ mode versus j for values of s closer to 1.

The second big surprise (at least to me), discussed in detail in [1], is that the infinite

series for the mode with $\omega = \omega_0$,

$$\psi_j(s) = \sum_{\ell=1}^{\infty} (-1)^{\ell-1} s^{(1-j)\ell} s^{-\ell(\ell+1)/2} (1 - s^{-\ell}) \left(\prod_{k=1}^{\ell} \frac{1}{(1 - s^{-k})^2} \right) \quad (2.3)$$

can be summed and expressed in terms of q -hypergeometric series¹ as follows²

$$\psi_j(s) = {}_1\phi_1\left(\{0\}, \{s\}, s, s^{1-j}\right) - {}_1\phi_1\left(\{0\}, \{s\}, s, s^{2-j}\right) \quad (2.4)$$

$$= -{}_1\phi_1\left(\{0\}, \{s^2\}, s, s^{2-j}\right) \quad (2.5)$$

For $s \gg 1$, in the mode with frequency ω_0 , the oscillation is localized near block 0, as expected, but as s gets closer to 1 it spreads out, as shown in figure 4. Because of the combination of scale invariance and translation invariance, all the modes are translated versions of the mode with $\omega = \omega_0$ — they all have the same shape. The mode with $\omega = s^{n/2}\omega_0$, is

$$\psi_j^n(s) = \psi_{j-n}(s) \quad (2.6)$$

Thus if the modes are normalized (and taken to be real), $\psi_j(s)$ satisfies

$$\sum_j \psi_j(s) \psi_{j-n}(s) = \delta_{0n} \quad (2.7)$$

Summing (2.7) over n gives another amusing result:

$$\left(\sum_j \psi_j(s) \right)^2 = 1 \quad (2.8)$$

We will proceed further along this direction in [1].

As s gets closer to 1, the modes spread out asymmetrically, as shown in figure 5. You might guess from the figures that the modes have a smooth continuum limit as j gets large for $s > 0$, and oscillate quickly to zero for sufficiently negative j . This is more or less correct. For very large j and s close to one, the solutions approach Bessel functions. To leading order in $(s - 1)$, these are the Bessel functions found in [7].

$$\frac{\sqrt{s^{-j}}}{s-1} \left(c_1 J_1 \left(\frac{2\sqrt{s^{-j}}}{s-1} \right) + 2ic_2 Y_1 \left(\frac{2\sqrt{s^{-j}}}{s-1} \right) \right) \quad (2.9)$$

The more accurate next order result in $(s - 1)$ is

$$- \frac{s^{3/2}}{\sqrt{2}} \sqrt{3s-5} \sqrt{s^{-j}} I_1 \left(\frac{2\sqrt{2}\sqrt{s^{-j}}}{(1-s)\sqrt{3s-5}} \right) \quad (2.10)$$

We will derive this and explore some subtleties in [1].

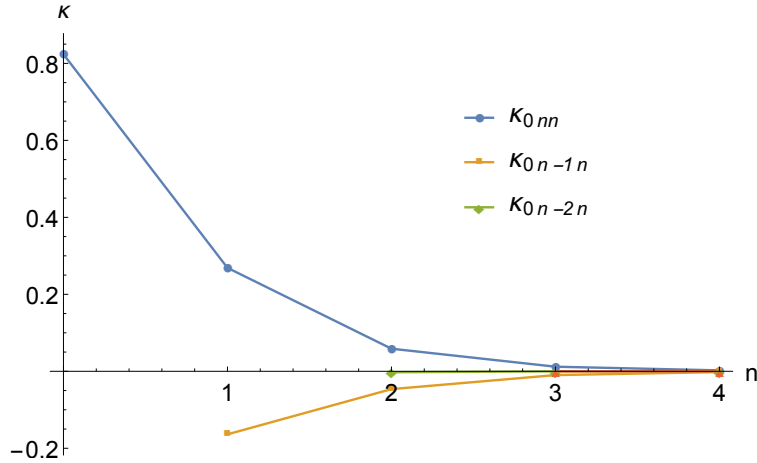


Figure 6: Delocalization of gauge couplings — Plots of $\kappa_{0n_1n_2}(s)$ for $s = 5$.

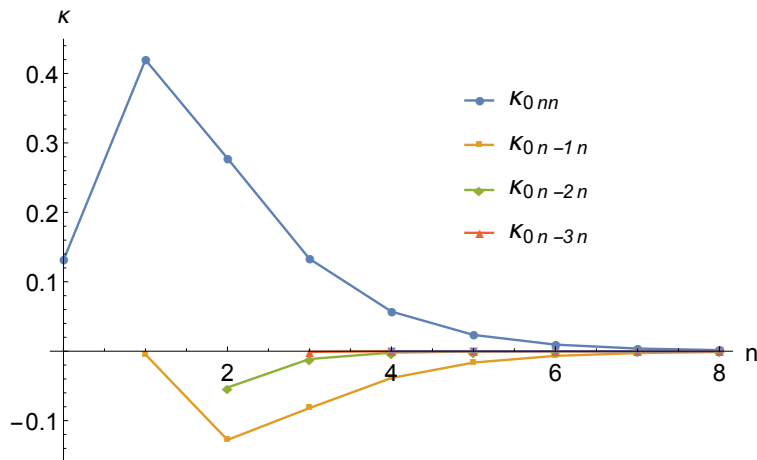


Figure 7: Delocalization of gauge couplings — Plots of $\kappa_{0n_1n_2}(s)$ for $s = 5/2$.

3 Gauge couplings

In the corresponding quantum field theory, at tree level, the wave functions of the massive vector bosons are related to the normal modes (2.6).

$$\mathcal{W}_n^\mu = \sum_j \psi_j^n(s) W_j^\mu = \sum_j \psi_{j-n}(s) W_j^\mu \quad (3.11)$$

where \mathcal{W}_n^μ is the field with mass $gvs^{n/2}$.

For large s , the state with mass gv has a wave functions that is localized around $j = 0$ — that is the mass eigenstate gauge field is approximately $\mathcal{W}_0^\mu \approx W_0^\mu$ with only a small admixture of the other fields.

¹I do not know whether this is related to the q -Bessel functions discussed in [10].

²The form (2.5) was obtained from (2.4) by Patrick Komiske

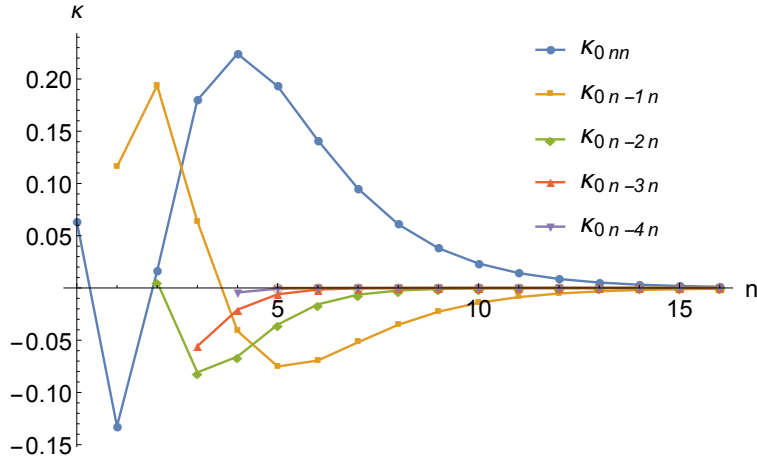


Figure 8: Delocalization of gauge couplings — Plots of $\kappa_{0n_1n_2}(s)$ for $s = 5/3$.

For s closer to 1, the wave functions of the mass eigenstates spread out, like the normal modes. The trilinear gauge couplings of the mass eigenstates for, n_1 , n_2 and n_3 are proportional to the symmetric tensor

$$\kappa_{n_1n_2n_3}(s) \equiv \sum_j \psi_{j-n_1}(s)\psi_{j-n_2}(s)\psi_{j-n_3}(s) \quad (3.12)$$

Because of the translation invariance of the modes, it is clear that only differences of the ns matter in (3.12).

Empirically, we find that the leading contribution to κ_{0jk} for $0 \leq j \leq k$ and large s has the form

$$\kappa_{0kk} = s^{-k} \quad \text{and} \quad \kappa_{0jk} = -s^{-(k-j)k} \quad \text{for } j < k \quad (3.13)$$

Note that the largest contribution, s^{-k} in (3.13) is of the order of the ratio of the scales between the mass eigenstates involved.

Figures 6, 7 and 8 show plots of $\kappa_{0n_1n_2}$. If s is not too close to 1, the couplings are largest when the two largest ns are equal and go exponentially zero if all the ns are very different.

The situation gets quite complicated for neighboring eigenstates as $s \rightarrow 1$. However, if we think about the “distance” between the mass eigenstates not in terms of lattice sites, but in terms of scale, we find that while spreading does occur as s get’s closer to 1, for sufficiently large scale difference, κ still falls like the square of ratio of the small mass to the large mass, just as in (3.13).

A nice way to see this is to plot $\text{Log}\left(\text{Abs}(\kappa_{0jk})\right)$ versus s^j and s^k , the ratios of the mass squares of the j and k eigenstates to the 0 eigenstate. Of course we lose the oscillating fine structure by taking the absolute value, but it allows us to take the logarithm and easily see the power dependence for large scale difference. This is shown in figure 9 for various values of s .³

³Note that while the three ridges in the plots look different, they all actually describe equivalent couplings

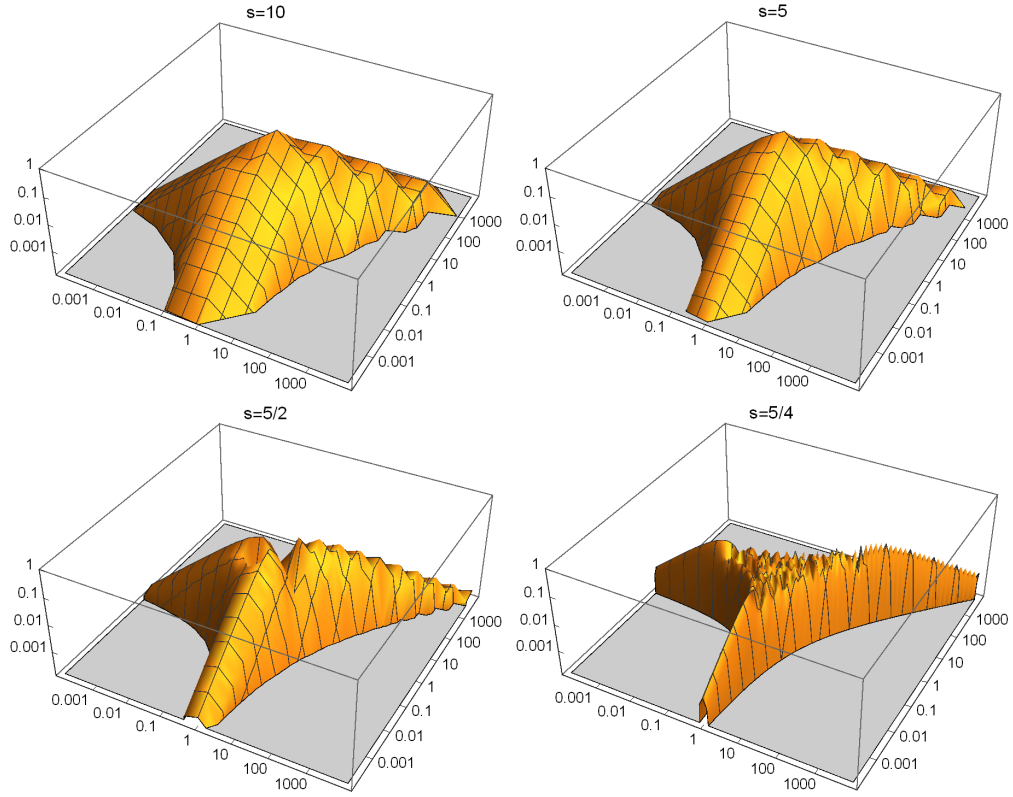


Figure 9: $\text{Log}(\text{Abs}(\kappa_{0jk}))$ versus s^j and s^k for various values of s

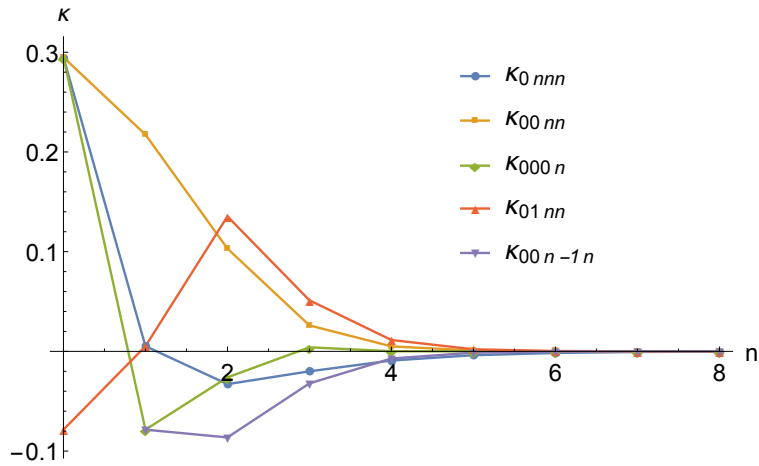


Figure 10: Delocalization of gauge couplings — Plots of $\kappa_{0n_1 n_2 n_3}(s)$ for $s = 5/2$.

because $\kappa_{0,j,j} = \kappa_{0,-j,0} = \kappa_{0,0,-j}$. The apparent difference is due to the plot on the rectangular grid which treats the ridge on the diagonal differently.

Similar delocalization occurs for the quartic couplings, proportional to

$$\kappa_{n_1 n_2 n_3 n_4}(s) \sum_j \psi_{j-n_1}(s) \psi_{j-n_2}(s) \psi_{j-n_3}(s) \psi_{j-n_4}(s) \quad (3.14)$$

Figure fig-spread-4-5-2 shows some components of (3.14) for $s = 5/2$. With more indices, the patterns are more difficult to characterize, but it is clear that the couplings are similarly spread out.

4 The tale of the missing photon

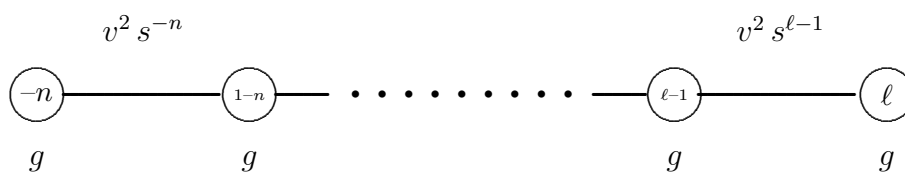


Figure 11: A truncated, finite version of the system in figure 2.



Figure 12: The mechanical analog of the finite system in figure 11.

If you think about the gauge symmetry of this system naively, you might be momentarily puzzled by the lack of a massless gauge field. The vacuum expectation values all preserve the “diagonal” gauge symmetry generated by the sum of all the individual generators. One might expect massless states corresponding to the unbroken gauge symmetry. We will refer to these as “photons” for short.

But we have seen that there are no massless states. The gauge bosons are all massive and associated with the normalizable normal modes, ψ_j^n . These form a complete basis for the space. The “would-be photon” has the non-normalizable wave function

$$\psi_j^\gamma = 1 \quad (4.15)$$

which has unit overlap with all the normal modes because of (2.8).

The physics becomes clear (if it is not already obvious) when you think about obtaining the infinite systems of figures 2 and 3 as the limit of the finite systems shown in figures 11 and 12. Now, obviously, in the mechanical system, there is a zero frequency mode in which all the blocks move together with wave function (4.15). And in the QFT, there is an unbroken

gauge symmetry with a gauge field proportional to

$$\sum_{j=-n+1}^{\ell+1} W_j^\mu \quad (4.16)$$

But the gauge coupling is

$$\frac{g}{\sqrt{n+\ell+1}} \quad (4.17)$$

which makes it clear what happens to the photon. As the system becomes infinite, the photon mode decouples and becomes unphysical. This is consistent with what we see in the infinite system.

5 The tail of the missing photon



Figure 13: A version of the system in figure 11 with variable boundary conditions.

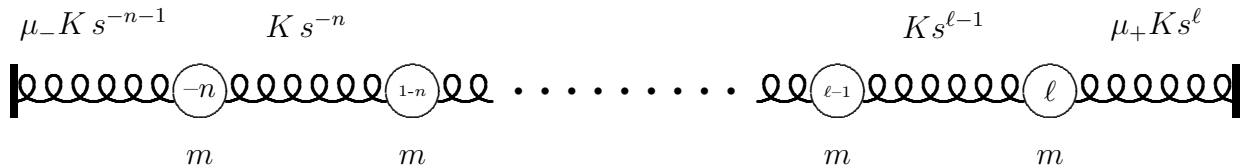


Figure 14: The mechanical analog of the system in figure 13.

The finite systems of figures 11 and 12 are more “physical” than the infinite systems of figures 2 and 3. We can actually build the mechanical system in figure 12. And the QFT in figure 11 is more realistic because it does not assume anything at arbitrarily large and small energy scales. On the other hand, the finite systems of figures 11 and 12 involve very specific assumptions about how things work at their boundaries, and it is worth generalizing this so we can study the very physical question of how things depend on boundary conditions. So in this section, we will study the systems shown in figures 13 and 14 in which the boundary conditions are variable. The mechanical system of figure 14 has springs at the end connected to fixed walls (the thick vertical lines) and the dimensionless parameters μ_{\pm} are the ratios of the actual spring constants to what we would have in the infinite system. The QFT analog

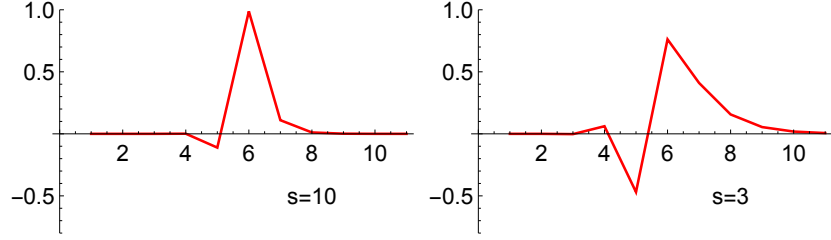


Figure 15: Modes of the infinite system.

figure 13 has variable VEVs at the ends and global rather than gauge symmetries at $j = \ell + 1$ and $-n - 1$.

We will study the normal modes of figure 14 as functions of the boundary parameters, μ_{\pm} . To begin, let us consider the form of the normal modes localized in the middle of the system. What we might expect from the exponential localization of the modes of the infinite system is that the effect of the boundary conditions on the central modes will be exponentially suppressed, of order

$$s^{-(\ell+n)/2} \quad (5.18)$$

And that is indeed how things work for the dependence on μ_- . We will illustrate this with

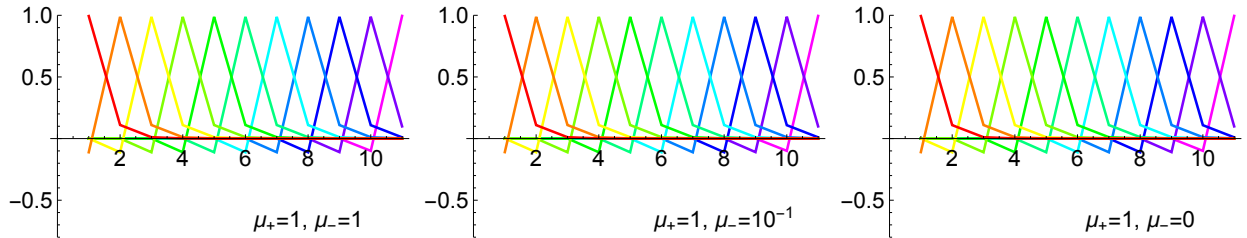


Figure 16: Dependence of the modes of the system in figure 14 on μ_- for $n + \ell = 10$, $s = 10$ and $\mu_+ = 1$.

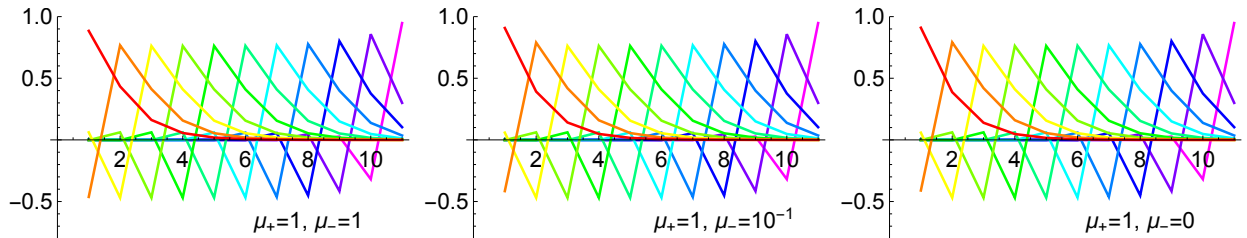


Figure 17: Dependence of the modes of the system in figure 14 on μ_- for $n + \ell = 10$, $s = 3$ and $\mu_+ = 1$.

three values of s , 10 and 3 which are well-enough localized that they fit comfortably into a finite system with $\ell + n = 10$, which is what we will use for illustration.

For $\mu_+ = 1$, you see in figures 16 and 17 that the effect of μ_- is tiny.⁴ You **can** see, particularly in figure 17, the effect of the boundaries on the nearby modes. Obviously, this effect increases as s gets closer to 1 and the modes spread out.

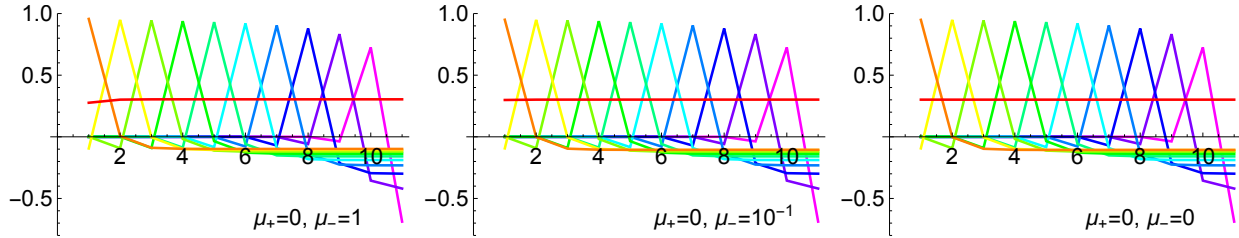


Figure 18: Dependence of the modes of the system in figure 14 on μ_- for $n + \ell = 10$, $s = 10$ and $\mu_+ = 0$.

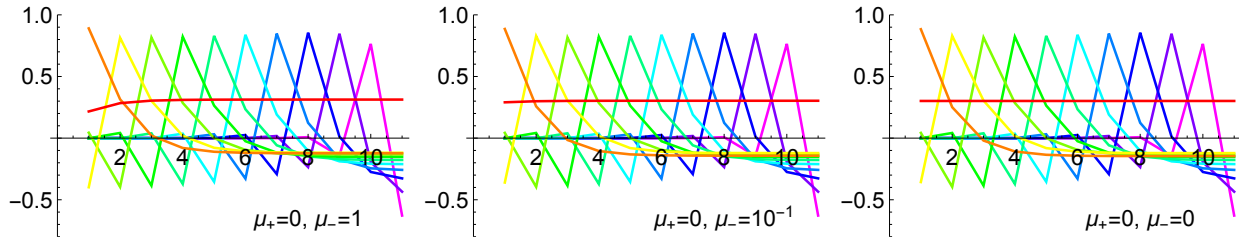


Figure 19: Dependence of the modes of the system in figure 14 on μ_- for $n + \ell = 10$, $s = 3$ and $\mu_+ = 0$.

For $\mu_+ = 0$, the analogous situation is shown in figures 18 and 19. Now there is a photon state for $\mu_- = 0$, so a very small μ_- can have a very large effect on the lowest mode. But for the rest of modes, the dependence on μ_- is too small to see. Note however, that the modes for $\mu_+ = 0$ look very different from the modes with $\mu_+ = 1$. This is the effect of the photon state (missing or not). It is worth pausing here to remark on why it makes such a big difference. It is helpful to look at the form of the modes for $\mu_- = \mu_+ = 0$ as $s \rightarrow \infty$. In this limit, it is easy to construct the modes by working down from the highest frequency mode and integrating out modes as we go down. The result is that the modes have the form

⁴In these and subsequent figures, the signs of the individual modes is ambiguous and I have chosen the signs to make the regularities apparent.

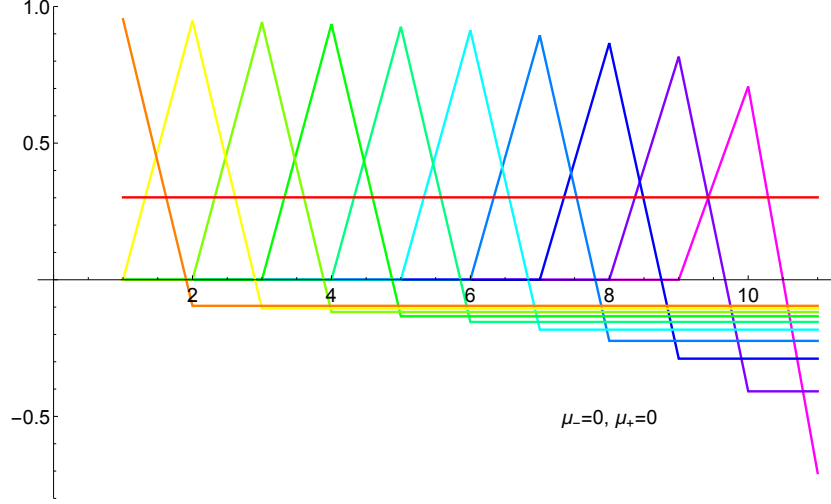


Figure 20: The modes of the system in figure 14 for $\mu_+ = \mu_- = 0$ for $n + \ell = 10$ as $s = \infty$.

(with $j = 1$ the highest frequency mode)

$$A_k^j = \begin{cases} 0 & \text{for } k < n + \ell + 1 - j \\ \sqrt{\frac{j}{j+1}} & \text{for } k = n + \ell + 1 - j \\ -\sqrt{\frac{1}{j(j+1)}} & \text{for } n + \ell + 1 - j < k \end{cases} \quad (5.19)$$

for $j = 1$ to $n + \ell$ and

$$A_k^{n+\ell+1} = \frac{1}{\sqrt{n + \ell + 1}} \quad \text{for all } k \quad (5.20)$$

where the lowest mode is the photon. This limiting form is shown in figure 20. If $n \rightarrow \infty$ and the system becomes semi-infinite, the modes in (5.19) are still valid, and in fact in this case they are the whole story because the photon mode goes missing in the limit $n \rightarrow \infty$. But for finite n and ℓ , (5.19) shows clearly how the modes manage to remain orthogonal to each other and to the photon mode. These modes are **mostly** localized about $k = n + \ell + 1 - j$, but they have a tail that stretches out to the upper boundary of the system.

We now turn to the case of μ_+ dependence for $\mu_- = 0$. You can see immediately from figures 21 and 22 that something much more interesting is going on in this case. To tease out what is going on, let's begin by plotting the just the lowest mode for $s = 10$. This is shown in figure 23. It is still hard to tell what is going on when the value gets close to zero, so we can take advantage of the fact that this mode does not change sign and use a log plot, as shown in figure 24.

Evidently, what is happening is that while for $\mu_+ = 1$, the mode decreases exponentially for all j , for smaller μ_+ , the mode decreases out to about $j = \ell + n + 1 + \log_{10} \mu_+$, and then it levels out and becomes “photon like”. This break occurs for j such that the local spring constant is of the order of the spring constant at the upper boundary. For larger j , the effect of the boundary spring is negligible compared to the local springs and the rest of the mode

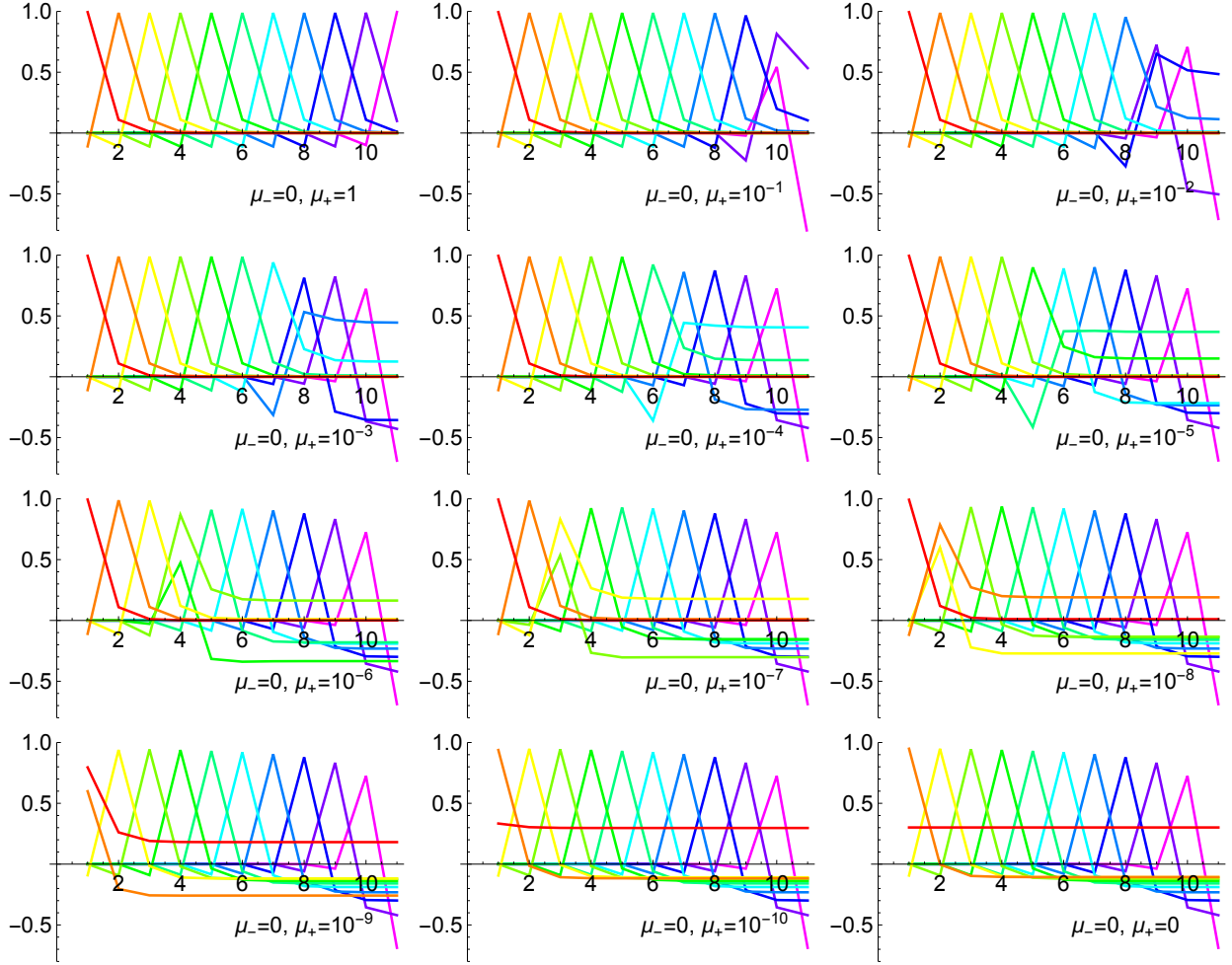


Figure 21: Dependence of the modes of the system in figure 14 on μ_+ for $n + \ell = 10$, $s = 10$ and $\mu_- = 0$.

looks photon-like. In this way, the lowest mode changes smoothly from the exponentially decreasing mode at $\mu_+ = 1$ to a photon-like constant mode for $\mu_+ < 10^{-10}$.

For general s , the break occurs for $j \approx \ell + n + 1 + \log_s \mu_+$. For larger j (smaller frequencies), the modes are localized and resemble the corresponding modes in figure 16 and 17. For smaller j (higher frequencies) the modes have a tail out to the right boundary and resemble the corresponding modes in figure 18 and 19.

6 Where's the physics?

In the infinite system, we have equivalent physics at every scale because we have built in scale invariance. And the physics is local in scale. Objects of a certain mass interact preferentially with objects of similar mass. We have seen in section 3 that the gauge couplings between

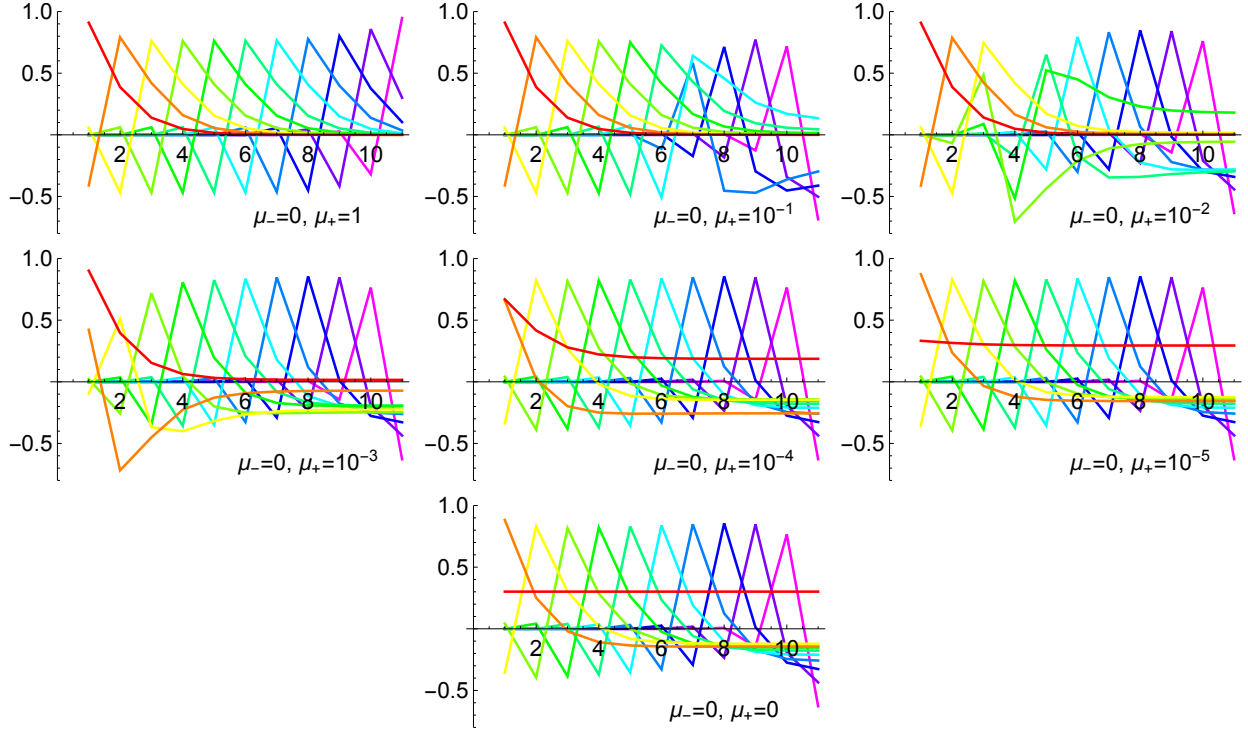


Figure 22: Dependence of the modes of the system in figure 14 on μ_+ for $n + \ell = 10$, $s = 3$ and $\mu_- = 0$.

heavy gauge fields with very different masses are power-law suppressed. This is what we might expect from effective field theory. Even as $s \rightarrow 1$, while the objects themselves spread out, the locality in scale persists at sufficiently large scales.

But the dependence on boundary conditions of the wave functions that we identified in section 5 is quite different. We have seen in the figures that the details of the boundary condition at the high scale has a dramatic effect on the structure of the low-energy end of the chain. The very existence of the photon is an obvious example, but in addition, the long tails of the other low-lying modes in figure 20 and the strong dependence of the low-lying modes on a small VEV at the large scale shown in figure 21 and 22. All of these effects are in some sense small. For the low lying modes, they are suppressed by a factor of the order of

$$\frac{1}{n + \ell} \tag{6.21}$$

But because the inverse of this factor is **linear** in the distance between in mode in term of number of sites, it is **logarithmic** in the ratio of large scale over the small scale. Thus these are effects of order

$$\frac{1}{n + \ell} = \frac{\text{Log}(s)}{\text{Log}(s^\ell/s^{-n})} = \frac{\text{Log}(s)}{\text{Log}(m_{\text{large}}^2/m_{\text{small}}^2)} \tag{6.22}$$

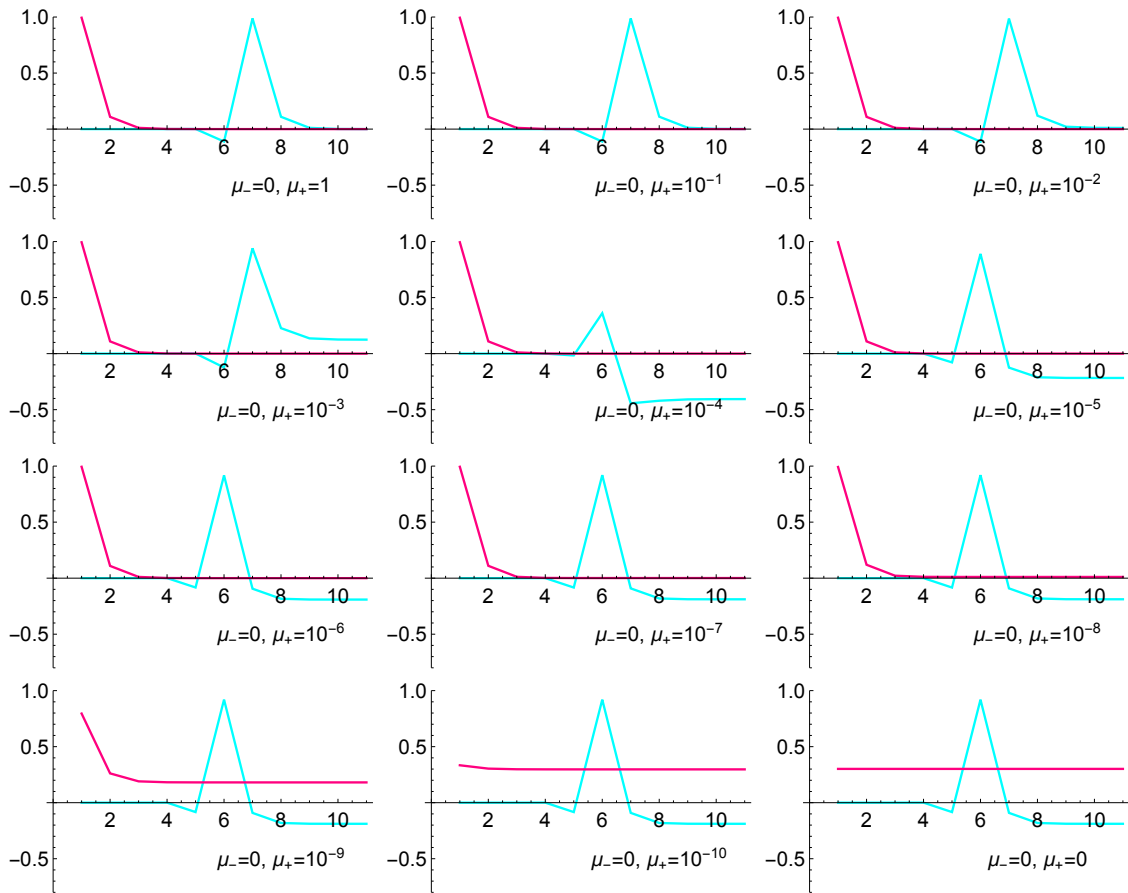


Figure 23:

I do not have any firm conclusions from this exercise, but I find (6.22) rather tantalizing. It looks like a violation of locality in scale that depends critically on the discreteness of the scale invariance in the model, because the effects are proportional to $\text{Log}(s)$ and disappear as $s \rightarrow 1$. I do not know how to construct models of this kind in a natural way, but I think that any sort of violation of standard effective field theory power counting is worth exploring further.

Acknowledgements

Matt Schwartz and Patrick Kamiske participated in early stages of this exploration and I am very grateful for many important discussions with them. Matt Reece was extremely helpful in pointing me to the literature on deconstructed AdS(5) and it is not his fault if I have left out important connections to this large body of work. I am also grateful to Jesse Thaler for suggestions. HG is supported in part by the National Science Foundation under grant PHY-1418114.

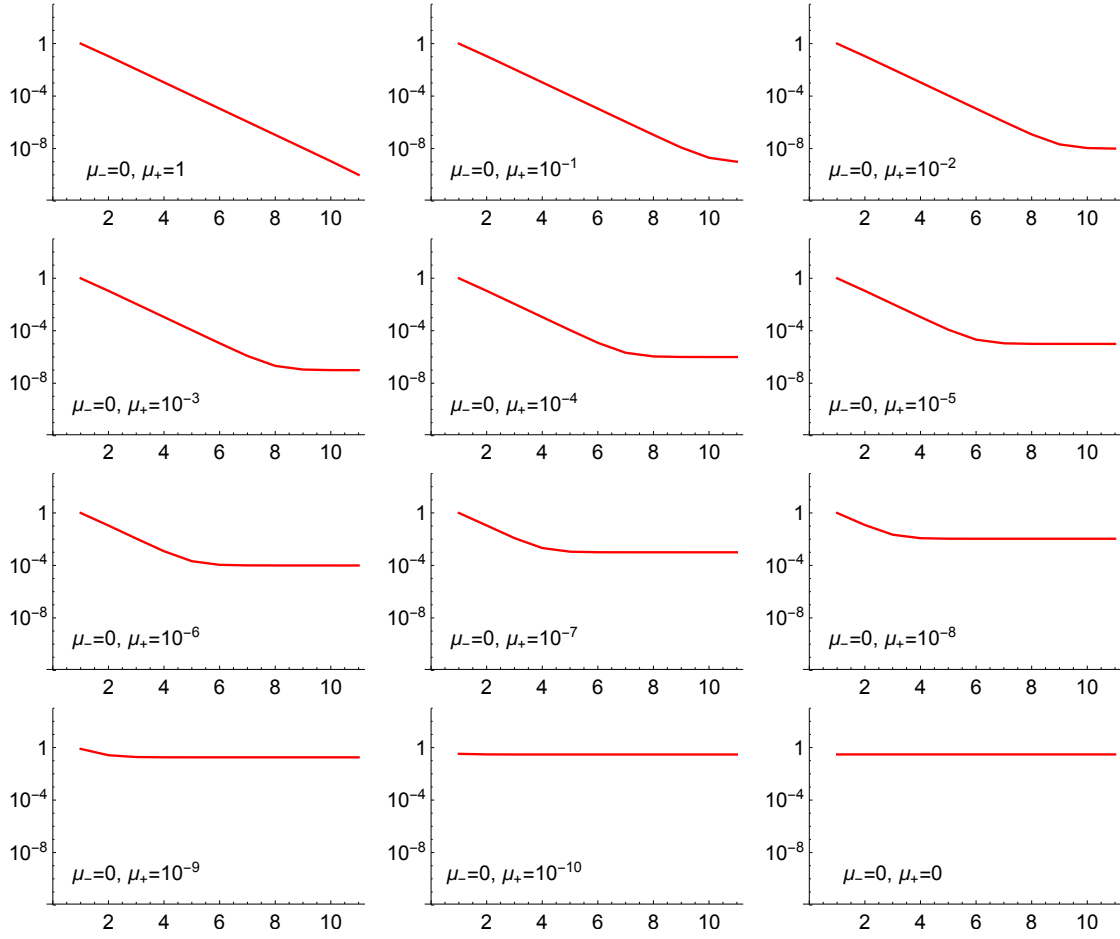


Figure 24:

References

- [1] H. Georgi, “Math Fun with Discrete Scale Invariance,”.
- [2] H.-C. Cheng, C. T. Hill, and J. Wang, “Dynamical electroweak breaking and latticized extra dimensions,” *Phys. Rev.* **D64** (2001) 095003, [arXiv:hep-ph/0105323](#) [hep-ph].
- [3] H. Abe, T. Kobayashi, N. Maru, and K. Yoshioka, “Field localization in warped gauge theories,” *Phys. Rev.* **D67** (2003) 045019, [arXiv:hep-ph/0205344](#) [hep-ph].
- [4] A. Katz and Y. Shadmi, “Gauge theories in AdS(5) and fine-lattice deconstruction,” *JHEP* **11** (2004) 060, [arXiv:hep-th/0409223](#) [hep-th].
- [5] A. Falkowski and H. D. Kim, “Running of gauge couplings in AdS(5) via deconstruction,” *JHEP* **08** (2002) 052, [arXiv:hep-ph/0208058](#) [hep-ph].

- [6] L. Randall, Y. Shadmi, and N. Weiner, “Deconstruction and gauge theories in AdS(5),” *JHEP* **01** (2003) 055, [arXiv:hep-th/0208120](#) [hep-th].
- [7] L. Randall, M. D. Schwartz, and S. Thambyahpillai, “Discretizing gravity in warped spacetime,” *JHEP* **10** (2005) 110, [arXiv:hep-th/0507102](#) [hep-th].
- [8] H. Georgi, “Fun with Higgsless theories,” *Phys. Rev.* **D71** (2005) 015016, [arXiv:hep-ph/0408067](#) [hep-ph].
- [9] N. Arkani-Hamed, A. G. Cohen, and H. Georgi, “Electroweak symmetry breaking from dimensional deconstruction,” *Phys. Lett.* **B513** (2001) 232–240, [arXiv:hep-ph/0105239](#) [hep-ph].
- [10] J. de Blas, A. Falkowski, M. Perez-Victoria, and S. Pokorski, “Tools for deconstructing gauge theories in AdS(5),” *JHEP* **08** (2006) 061, [arXiv:hep-th/0605150](#) [hep-th].